

# ALMA Memo 494

14 May 2004

## MF-112 AND MF-116: COMPACT WAVEGUIDE LOADS AND FTS MEASUREMENTS AT ROOM TEMPERATURE AND 5 K

A. R. Kerr<sup>†</sup>, H Moseley<sup>\*</sup>, E. Wollack<sup>\*</sup>, W. Grammer<sup>‡</sup>, G. Reiland<sup>‡</sup>, R. Henry<sup>\*</sup>, K.P. Stewart<sup>\*\*</sup>

### INTRODUCTION

In many applications it is convenient to have a compact waveguide load which is well matched but occupies a minimum of space. In this memo we describe measurements on waveguide loads of the three configurations shown in Fig. 1, and also Fourier transform spectrometer (FTS) measurements on samples of the Eccosorb MF-112 and MF-116 absorbing materials [1] used for these loads. The dimensions in Fig. 1 are for WR-10 (75-110 GHz) loads, but the design can be scaled for any band. These loads are compact in comparison with a typical commercial load of the corner wedge type which is ~1.2" long for WR-10 waveguide.

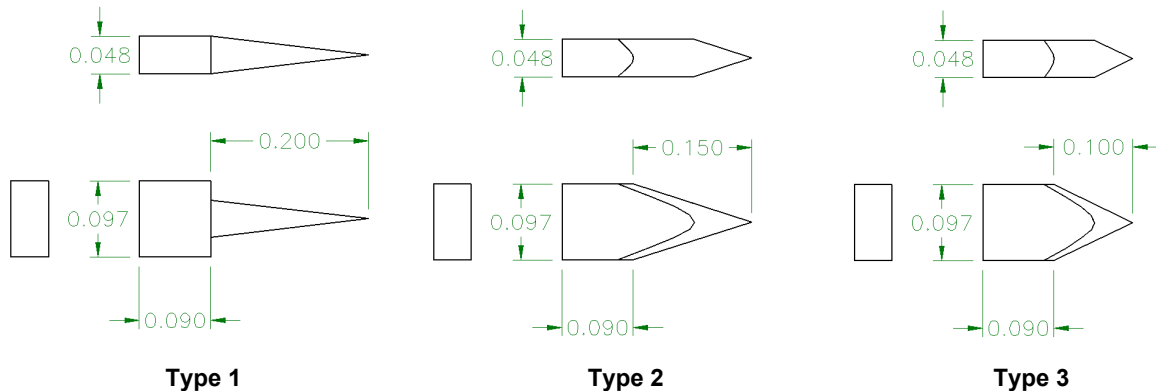


Fig. 1. Three compact waveguide loads. The dimensions, in inches, are for WR-10 waveguide, but they can be scaled to any band.

### ROOM TEMPERATURE MEASUREMENTS OF WAVEGUIDE LOADS

#### 75-110 GHz Measurements

Loads of types 1, 2, and 3 for WR-10 waveguide were made of MF-112 and MF-116 material and measured on an HP8510 vector network analyzer. After calibrating the VNA, the load under test was inserted in the waveguide and its two-port S-parameters measured. Results

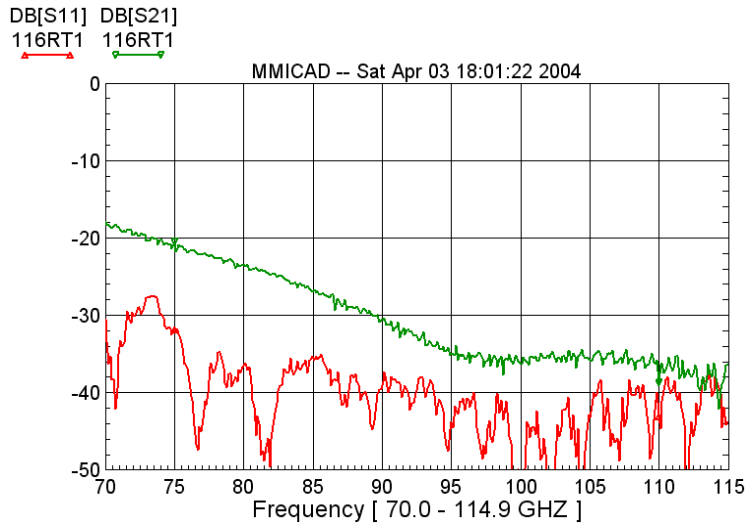
<sup>†</sup> National Radio Astronomy Observatory, Charlottesville, VA 22903.

<sup>\*</sup> Goddard Space Flight Center, Greenbelt, MD 20771.

<sup>‡</sup> National Radio Astronomy Observatory, Tucson, AZ 85721.

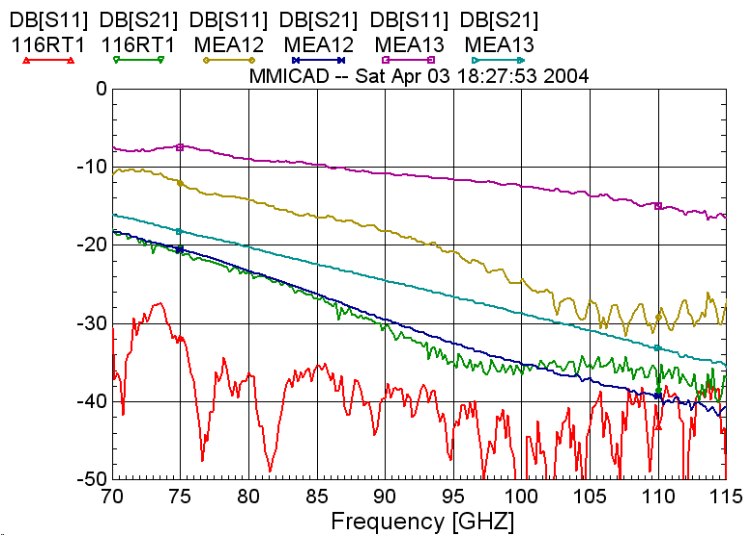
<sup>\*\*</sup> Naval Research Laboratory, Washington, DC 20375

for a typical MF-116 Type 1 load are shown in Fig. 2. The return loss is greater than 30 dB over the waveguide band (75-110 GHz), and the transmission loss is greater than 20 dB. Loads of Types 1, 2, and 3 are compared in Fig. 3. It is clear that the Type 2 and 3 loads are not as well matched to the waveguide as the Type 1 load.



**Type 1 WR-10 load  
MF-116  
293 K**

**Fig. 2. VNA measurements of  $S_{11}$  (red) and  $S_{21}$  (green) in dB of a WR-10 Type 1 MF-116 load. (At room temperature.)**

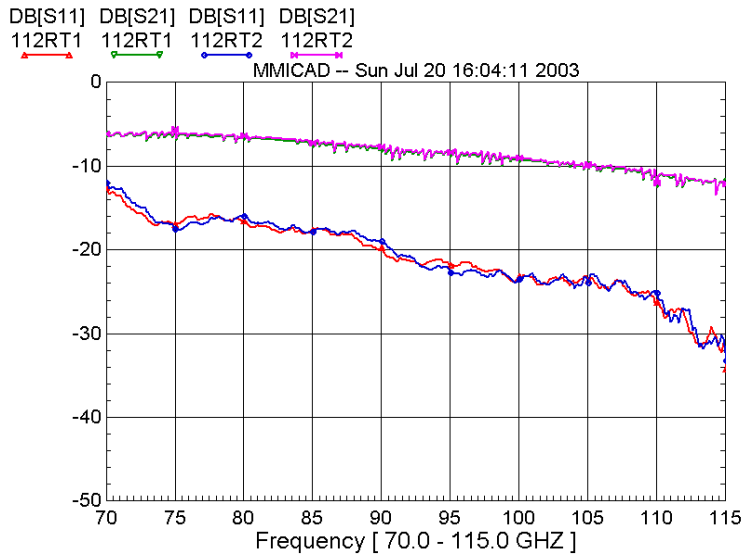


**Type 1, 2, & 3 WR-10 loads  
MF-116  
293 K**

**Fig. 3. VNA measurements of  $S_{11}$  and  $S_{21}$  in dB of MF-116 WR-10 loads of Types 1, 2, and 3. (At room temperature.)**

**Type 1:  $S_{11}$  red,  $S_{21}$  green  
Type 2:  $S_{11}$  brown,  $S_{21}$  dark blue  
Type 3:  $S_{11}$  magenta,  $S_{21}$  light blue**

Similar measurements were made on two Type-1 loads made of MF-112. These are shown in Fig. 4. In the lower part of the WR-10 band the return loss is as low as 16 dB and the transmission loss is as low as 6 dB — clearly inferior to the MF-116 load of the same geometry. If such a load were used in a blind waveguide (*i.e.*, with a metal wall behind the load), -12 dB of the input power would be reflected back to the source from the blind end of the waveguide and would interfere with the -16 dB direct reflection ( $S_{11}$ ), giving net return loss minima as low as 8 dB.

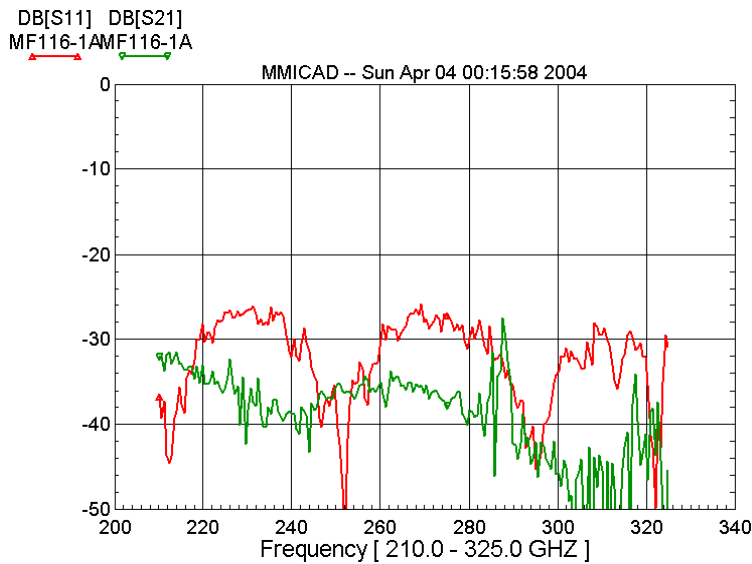


**Type 1 WR-10 loads  
 MF-112  
 293 K**

**Fig. 4. VNA measurements of  $S_{11}$  (lower curves) and  $S_{21}$  (upper curves) in dB for two WR-10 Type 1 MF-112 loads. (At room temperature.)**

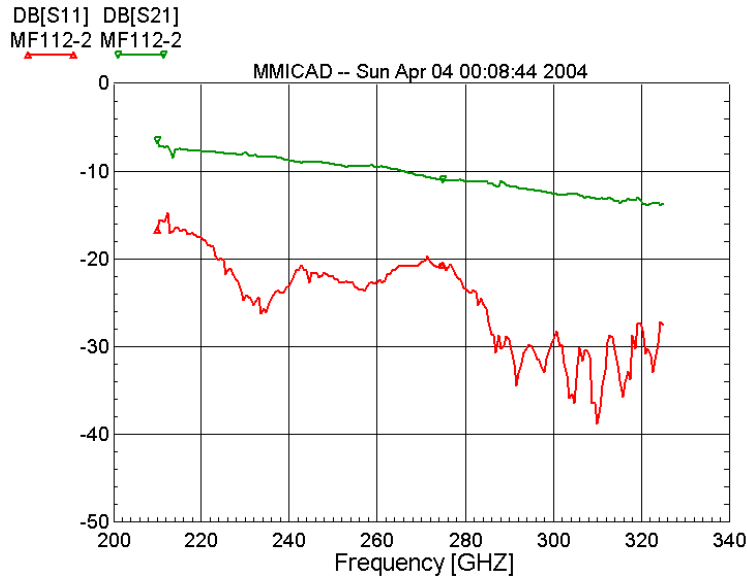
**220-325 GHz Measurements**

MF-112 and MF-116 Type 1 loads were made for WR-3.7 waveguide by scaling the dimensions in Fig. 1. They were measured on a HP8510 vector network analyzer with Oleson WR-3.4 extender modules and appropriate waveguide transitions. The results are shown in Figs. 5 and 6. Only room temperature measurements were made in this waveguide band.



**Type 1 WR-3.7 load  
 MF-116  
 293 K**

**Fig. 5. VNA measurements of  $S_{11}$  (red) and  $S_{21}$  (green) in dB of a WR-3.7 Type 1 MF-116 load. (At room temperature.)**

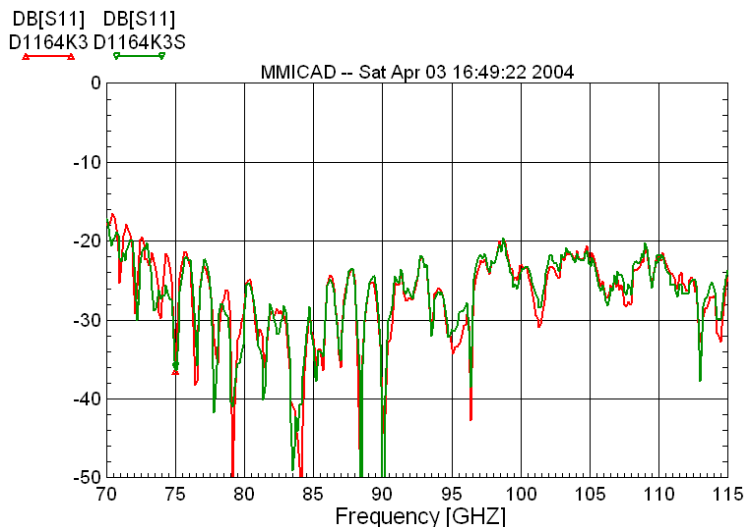


**Type 1 WR-3.7 load  
MF-112  
293 K**

**Fig. 6. VNA measurements of  $S_{11}$  (red) and  $S_{21}$  (green) in dB of a WR-3.7 Type 1 MF-112 load. (At room temperature.)**

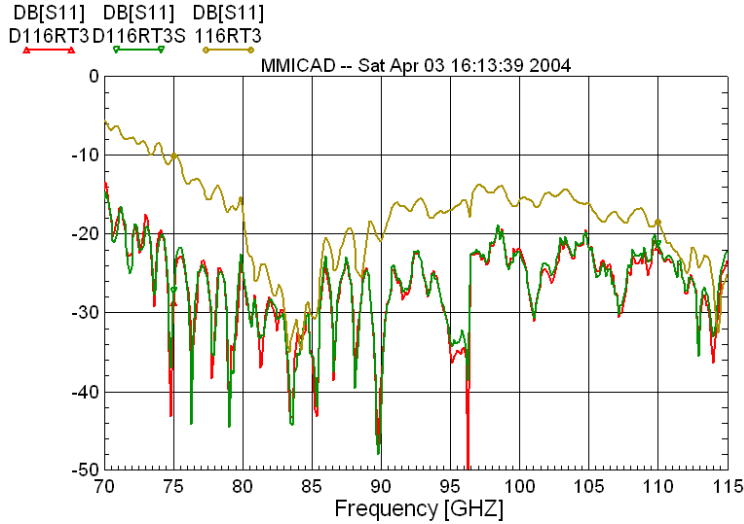
### MEASUREMENT OF WR-10 WAVEGUIDE LOADS AT 4 K

To measure the return loss of the MF-112 and MF-116 WR-10 Type 1 loads at 4 K, they were mounted in a waveguide inside a liquid helium cooled vacuum cryostat. As the waveguide vacuum window was not well matched over the full waveguide band, it was measured separately on the VNA and de-embedded from the load measurements using MMICAD v2. The 4-K results are shown in Figs. 7 and 9. For comparison, Figs. 8 and 10 show room temperature measurements of the same loads in the cryostat. A measurement without de-embedding the vacuum window is included in Fig. 8. The ripples in Figs. 7-10, with a period of  $\sim 1.5$  GHz, correspond to a reflection at the -30 dB level at the warm end of the waveguide inside the cryostat interfering with the reflection from the load under test.



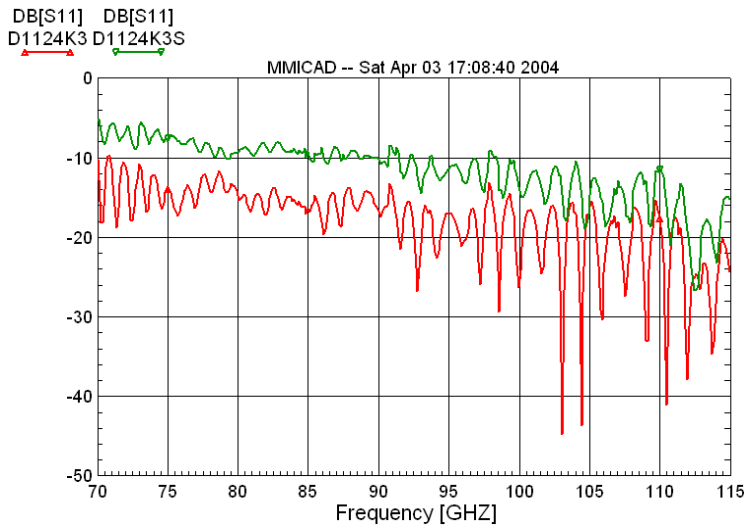
**Type 1 WR-10 load  
MF-116  
4 K**

**Fig. 7.  $S_{11}$  (dB) for the WR-10 MF-116 Type 1 load at 4 K. The red curve is with a second load behind the load under test, and the green curve is with a short circuit behind the load under test.**



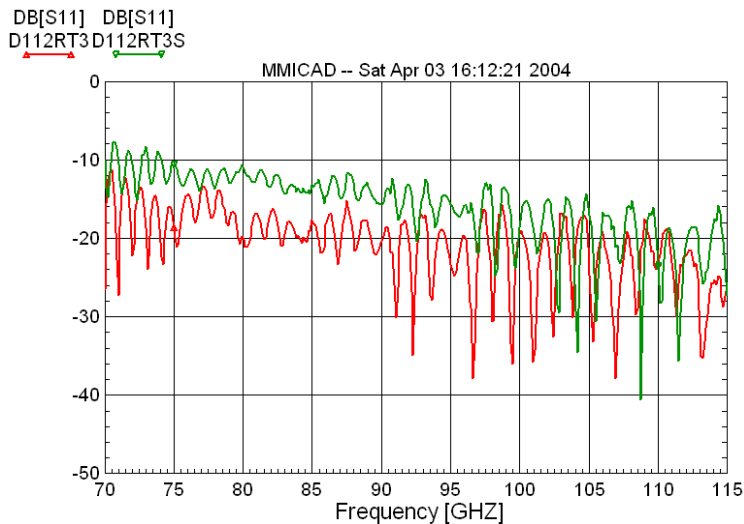
**Type 1 WR-10 load  
MF-116  
293 K**

Fig. 8. For comparison with Fig. 5,  $S_{11}$  (dB) for the WR-10 MF-116 Type 1 load at room temperature, measured in the cryostat. The lower curves are (red) with a second load behind the load under test, and (green) with a short circuit behind the load under test. The upper curve (brown) is with a second load behind the load under test but without de-embedding the vacuum window.



**Type 1 WR-10 load  
MF-112  
4 K**

Fig. 9.  $S_{11}$  (dB) for the WR-10 MF-112 Type 1 load at 4 K. The red curve is with a second load behind the load under test, and the green curve is with a short circuit behind the load under test.



**Type 1 WR-10 load  
MF-112  
293 K**

Fig. 10. For comparison with Fig. 7.  $S_{11}$  (dB) for the WR-10 MF-112 Type 1 load at room temperature, measured in the cryostat. The red curve is with a second load behind the load under test, and the green curve is with a short circuit behind the load under test.

## FTS MEASUREMENTS OF MF-112 AND MF-116 AT 300 K AND 5 K

Samples of MF-112 and MF-116 of diameter 1 inch were measured at room temperature and 5 K using the Bruker IFS113V Fourier transform spectrometer at Goddard Space Flight Center. For our MF-112 and MF-116 samples, at low frequencies where the attenuation is not too large, ripples occur in the transmission vs frequency plot. The period of the ripples depends on the length of the sample and on the phase constant of the material, while the amplitude of the ripples depends on the characteristic impedance of the material (which governs the reflection coefficient at each end of the sample) and its attenuation. It will be seen from the results below that the measured data are well characterized by an attenuation constant which is quadratic in frequency, a frequency-independent characteristic impedance, and a frequency-independent effective dielectric constant which embodies both the dielectric and magnetic terms of the phase constant<sup>1</sup>. The microwave circuit simulator MMICAD v2 was used to fit the parameters of a lossy transmission line to the measured transmittance data over the frequency range in which the data did not have appreciable noise. The attenuation constant  $A = A_1 f + A_2 f^2$  ( $f$  is in GHz) has units of dB/m, and the characteristic impedance  $Z$  and the effective dielectric constant  $K$  are both relative to free space.

### FTS Measurements of MF-116

Figs. 11 and 12 show FTS measurements of the transmission of 0.010" and 0.005" samples of MF-116 at room temperature (red curves). Also shown (green curves) are the best fit model transmission with the parameters listed in the figure caption. Fig. 13 shows the same information for the 0.005" sample at 5 K.

### FTS Measurements of MF-112

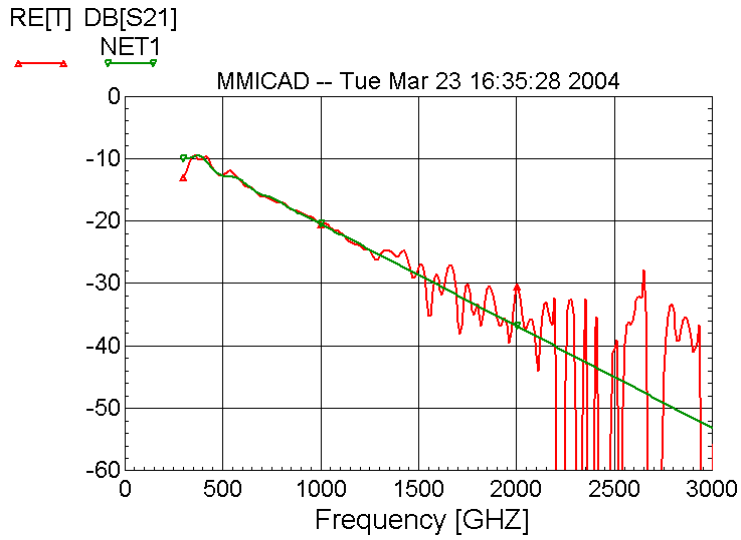
Figs. 14 and 15 show FTS measurements of the transmission of 0.040" and 0.020" samples of MF-112 at room temperature (red curves). Also shown (green curves) are the best fit model transmission with the parameters listed in the figure caption. Fig. 16 shows the same information for the 0.020" sample at 5 K.

---

<sup>1</sup> Propagation in the medium is governed by the wave impedance  $Z_c$  and the propagation constant  $\gamma$ , both of which are complex and depend on the complex permittivity  $\epsilon'(1 + j \tan(\delta_d))$  and permeability  $\mu'(1 + j \tan(\delta_m))$ :

$$Z_c = \sqrt{\frac{\mu'(1 + j \tan \delta_m)}{\epsilon'(1 + j \tan \delta_d)}}, \quad \gamma = \sqrt{-\left[\mu'(1 + j \tan \delta_m)\right]\left[\epsilon'(1 + j \tan \delta_d)\right]}.$$

The equivalent lossy transmission line to which the FTS data are fitted in Figs. 11-16 is characterized by its characteristic impedance  $Z$ , attenuation constant  $A$ , and effective dielectric constant  $K$ . The relationship between material parameters and the transmission line parameters is:  $Z = |Z_c|$ ,  $A = \text{Re}[\gamma]$  and  $K = (\text{Im}[\gamma])^2 / \epsilon_0 \mu_0$ .



**MF-116**  
**0.010"**  
**293 K**

Fig. 11. Transmission (dB) of a 0.010" sample of MF-116 at room temperature.

Red curve: FTS measurement

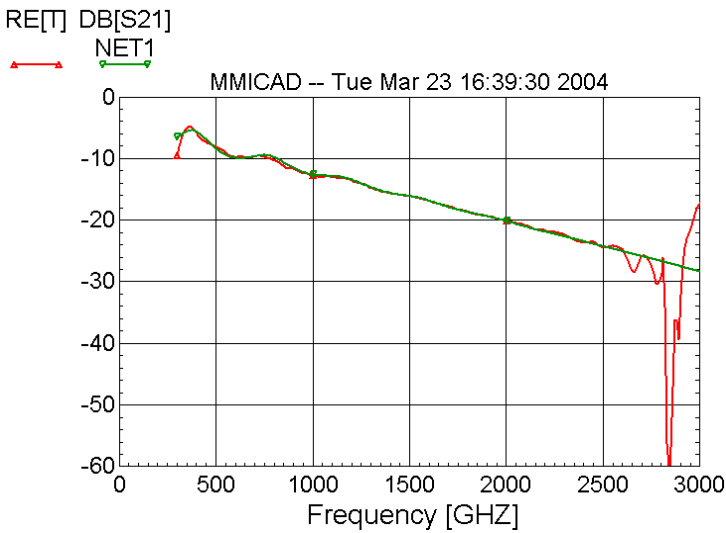
Green curve: model fit with

$$A_1 = 64.4$$

$$A_2 = 0$$

$$K = 9.0$$

$$Z = 0.24$$



**MF-116**  
**0.005"**  
**293 K**

Fig. 12. Transmission (dB) of a 0.005" sample of MF-116 at room temperature.

Red curve: FTS measurement

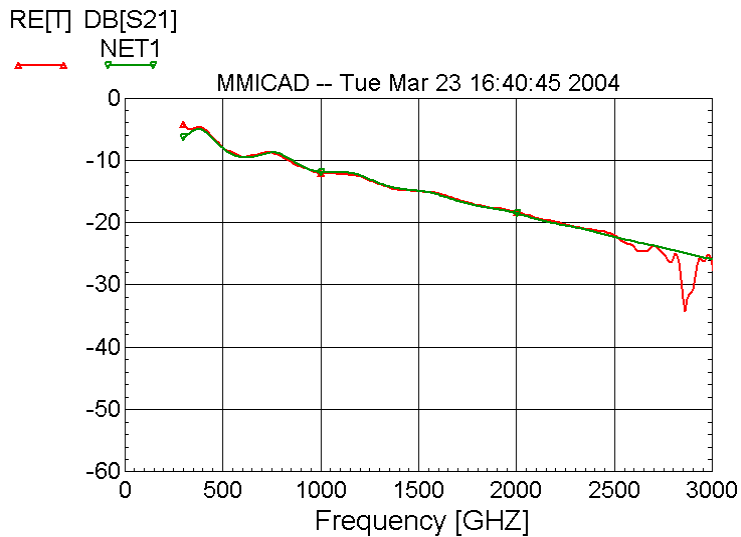
Green curve: model fit with

$$A_1 = 63.5$$

$$A_2 = 0$$

$$K = 9.0$$

$$Z = 0.24$$



**MF-116**  
**0.005"**  
**5 K**

Fig. 13. Transmission (dB) of a 0.005" sample of MF-116 at 5 K.

Red curve: FTS measurement

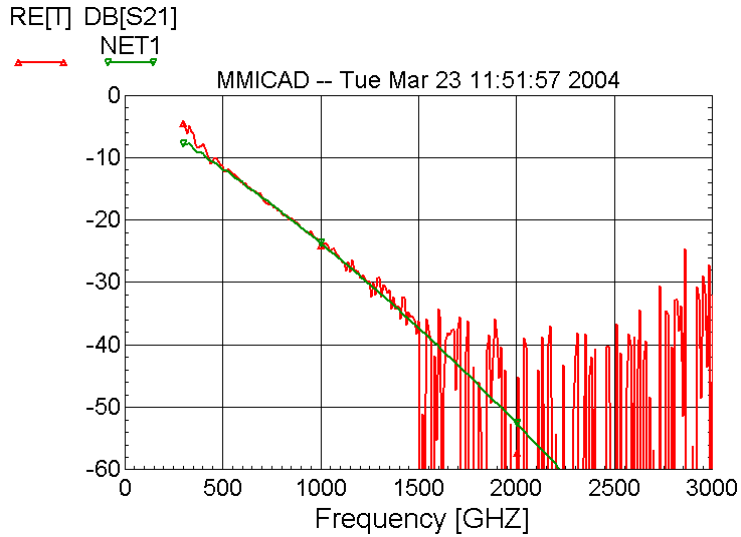
Green curve: model fit with

$$A_1 = 57.3$$

$$A_2 = 0$$

$$K = 9.0$$

$$Z = 0.24$$



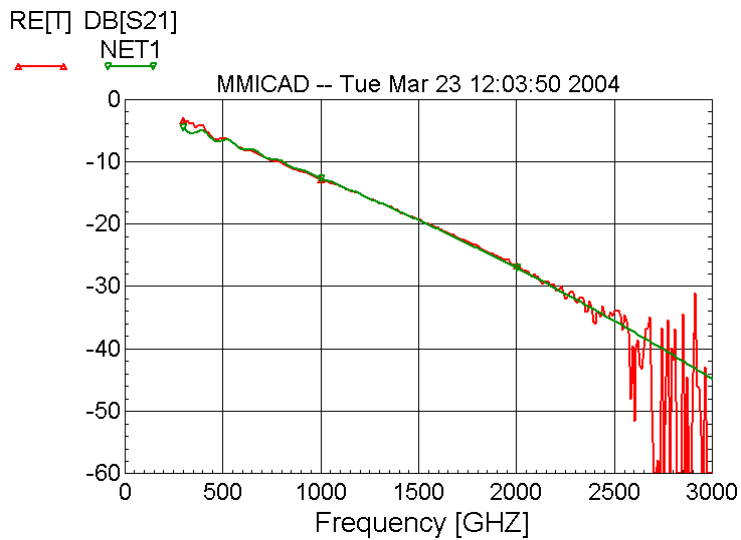
**MF-112**  
**0.040"**  
**293 K**

Fig. 14. Transmission (dB) of a 0.040" sample of MF-112 at room temperature.

Red curve: FTS measurement

Green curve: model fit with

$A_1 = 18.5$   
 $A_2 = 0.0033$   
 $K = 4.9$   
 $Z = 0.43$



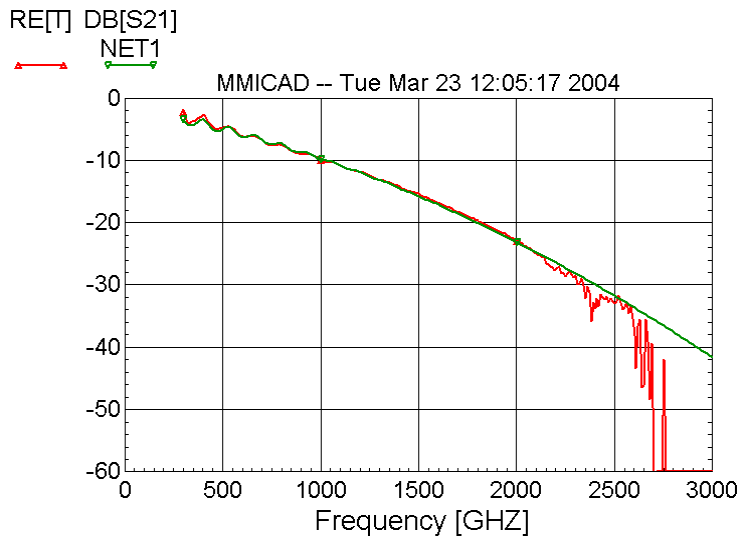
**MF-112**  
**0.020"**  
**293 K**

Fig. 15. Transmission (dB) of a 0.020" sample of MF-112 at room temperature.

Red curve: FTS measurement

Green curve: model fit with

$A_1 = 18.5$   
 $A_2 = 0.0033$   
 $K = 4.9$   
 $Z = 0.43$



**MF-112**  
**0.020"**  
**5 K**

Fig. 16. Transmission (dB) of a 0.020" sample of MF-112 at 5 K.

Red curve: FTS measurement

Green curve: model fit with

$A_1 = 11.1$   
 $A_2 = 0.0051$   
 $K = 4.9$   
 $Z = 0.43$

## DISCUSSION & CONCLUSIONS

### Compact Waveguide Loads

It is clear from the results in Figs. 2-6 that the Type 1 compact load is superior to the Type 2 and 3 loads. The Type 1 load is about one quarter of the length of a typical commercial waveguide load and, when made of MF-116, it has a return loss > 30 dB over the full WR-10 band (75-110 GHz) and > 27 dB over the WR-3.7 band (200-300 GHz) at room temperature.

The limitations of the waveguide 4 K measurement setup enabled us only to determine that the return loss of the WR-10 MF-116 load was > 20 dB. However, based on the observation that the material properties measured by FTS at room temperature and 5 K differ only slightly, the return loss of the Type 1 MF-116 load at cryogenic temperatures should be similar to the room temperature values.

Cryogenic measurements of the WR-3.7 MF-116 waveguide loads were not made but, based on the material properties measured by FTS, they too should have a return loss at low temperatures close to the room temperature values.

### Material Properties

While the FTS data in Figs. 11-16 are plotted over the frequency range 300-3000 GHz, the results below ~400 GHz are of questionable accuracy. This is because the finite étendue of the FTS limits the calibration accuracy at the lowest frequencies. At high frequencies, the measurement accuracy is limited by the dynamic range of the detector on the FTS. The data were fitted to a simple lossy transmission line characterized by its characteristic impedance  $Z$ , attenuation constant  $A = A_1 f + A_2 f^2$  ( $f$  is in GHz) dB/m, and effective dielectric constant  $K$ .  $Z$  and  $K$  are both relative to free space. It was found that the transmission line characteristic impedance and effective dielectric constant were independent of frequency for each material. Table I shows the best fit values from Figs. 11-16.

**TABLE I**

Material	Temperature	Characteristic Impedance <sup>a</sup>	Effective Dielectric Constant <sup>a</sup>	Attenuation <sup>b</sup> $A = A_1 f + A_2 f^2$ dB/m	
		$Z$	$K$	$A_1$	$A_2$
MF-112	293 K	0.43	4.9	18.5	0.0033
	5 K	0.43	4.9	11.1	0.0051
MF-116	293 K	0.24	9.0	64.0	0
	5 K	0.24	9.0	57.3	0

a:  $Z$  and  $K$  are relative to free space.

b:  $f$  is in GHz.

The material properties deduced from the FTS measurements are generally consistent with earlier measurements by Hemmati *et al.* [3] on the Emerson & Cuming CR series of materials room temperature and 80 K. The CR materials are castable versions of the MF materials (which are supplied as solid stock). Measurements of CR-110 at 1.2 K by Peterson and Richards [4] are consistent with those in [3].

The MF-112 FTS data used here are the same as used in ALMA Memo 273 [2]. The slight difference between the parameters deduced here for MF-112 and those in Memo 273 is a result of (i) the assumption in Memo 273 that the characteristic impedance (relative to free space) is simply  $1/\sqrt{\epsilon_r}$ , while in the present work it is a free parameter, and (ii) a different weighting of the optimization parameters. The present results give better agreement between the FTS data and the transmission line model.

### REFERENCES

- [1] Emerson & Cuming Microwave Products, Randolph, MA 02368, <http://www.eccosorb.com>
- [2] G.A. Ediss, A.R. Kerr, H. Moseley, K.P. Stewart, "FTS Measurements of Eccosorb MF112 at Room Temperature and 5 K from 300 GHz to 2.4 THz," ALMA Memo 273, 8 Sep. 1999. <http://www.alma.nrao.edu/memos/>.
- [3] H. Hemmati, J. C. Mather, and W. L. Eichhorn, "Submillimeter and millimeter wave characterization of absorbing materials," *Applied Optics*, vol. 24, no. 24, pp. 4489-4492, 15 Dec. 1985.
- [4] J. B. Peterson and P. L. Richards, "A cryogenic blackbody for millimeter wavelengths," *Int. J. Infrared & Millimeter Waves*, vol. 5, no. 12, pp. 1507-1515, 1984.